Comparison of Modulated Impurity-Concentration InP Transferred Electron Devices for Power Generation at Frequencies Above 130 GHz

Rolf Judaschke, *Member, IEEE*

***Abstract*—In this paper, InP transferred electron devices of various doping profiles have been theoretically investigated for fundamental- and harmonic-mode operation at frequencies up to 260 GHz. The results are based on an efficient and accurate hydrodynamic simulator, which analyzes the device under both conditions: impressed terminal voltage and realistic load impedances. In comparison with state-of-the-art graded profile diodes, improved performance is demonstrated for modulated impurity-concentration devices for both modes of operation.**

***Index Terms*—Gunn devices, harmonic-mode operation, modulated impurity-concentration devices.**

I. Introduction

At millimeter-wave frequencies, there is a growing interest in low-noise solid-state oscillators for applications in transmitters of high-resolution radars, as local oscillators, and as drivers for multipliers. Typical state-of-the-art RF output power levels of different types of Gunn and IMPATT oscillators are depicted in Fig. 1. InP Gunn devices operating in the fundamental and second harmonic mode have been shown to be suitable for the generation of low-noise oscillations at frequencies up to 170 GHz [3], [4]. However, the performance of Gunn oscillators at higher frequencies is still limited (e.g., less than 1-mW output power beyond 250 GHz [1], [2]). Thus, for power generation at frequencies above 170 GHz in most applications, either multipliers or silicon IMPATT oscillators are used, although the latter exhibit poor phase noise characteristics. In this contribution, the performance of InP Gunn devices in both fundamental- and harmonic-mode operation is theoretically investigated by a hydrodynamic (HD) device simulator. Special emphasis is attached to the influence of different doping profiles, as well as to the harmonic-mode driving voltage-to-phase relationship in order to optimize output power and device impedance.

II. Hydrodynamic Device Model

Due to the small characteristic device dimensions, nonstationary transport effects become significant in the millimeter-wave range. Thus, the drift–diffusion (DD) equations are inappropriate and, instead, HD models, Monte Carlo (MC) methods, or cellular-automaton (CA) particle simulations [5] are applied. Contrary to the well-known MC method, the CA method replaces the evaluation of the different single-scattering events by a "super-scattering" concept, which significantly increases the numerical efficiency of the transport simulation. Nevertheless, the drawback of both statistical methods is their computational effort, in particular, for consistent simulations when the oscillator load impedance characteristic must be included in the analysis. Thus, as a compromise between accuracy and computational efficiency, the HD model has been applied in this study.

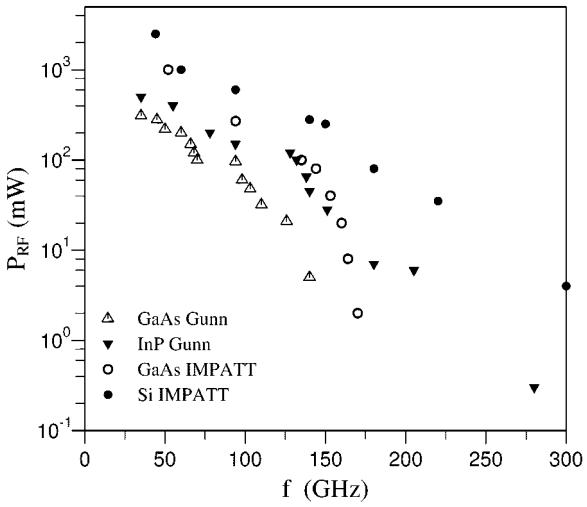

Fig. 1. Published continuous-wave output power levels of state-of-the-art millimeter-wave solid-state oscillators.

The HD transport equations are similar to those originally proposed in [6]. For unipolar carrier transport, they can be expressed as

$$\frac{\partial n}{\partial t} = -\nabla n\vec{v} + \left(\frac{\partial n}{\partial t}\right)_{\text{coll}} \tag{1}$$

$$\frac{\partial n\vec{v}}{\partial t} = -\frac{qn\vec{E}}{m} - \frac{1}{m}\nabla nk_BT + \left(\frac{\partial n\vec{v}}{\partial t}\right)_{\text{coll}} \tag{2}$$

$$\frac{\partial nw}{\partial t} = -qn\vec{v}\vec{E} - \nabla n\vec{S} + \left(\frac{\partial nw}{\partial t}\right)_{\text{coll}} \tag{3}$$

where n, $\vec{v}$, $\vec{E}$, w, and $\vec{S}$ are the electron density, velocity, electric field, energy, and energy flux, respectively. In comparison with the original equations, a different definition of the thermal

Manuscript received March 1, 1999.

The author is with the Arbeitsbereich Hochfrequenztechnik, Technische Universität Hamburg-Harburg, D-21071 Hamburg, Germany.

Publisher Item Identifier S 0018-9480(00)02531-X.

energy and a consistent treatment of the diffusive energy flow $\vec{Q}$ (also referred to as the heat flow) has been applied [7], which results in the auxiliary equations

$$w = \frac{3}{2} k_B T \tag{4}$$

$$\vec{S} = \frac{5}{3} \vec{v} w + \vec{Q} \tag{5}$$

$$\vec{Q} = -\lambda \nabla T \tag{6}$$

Both modifications are in coincidence with physical considerations and eliminate most of the instability problems that have been observed in other studies. The heat conduction coefficient λ is expressed as

$$\lambda = \frac{5}{2} \frac{\mu(E_{\rm ss}) k_B^2 T}{q}. \tag{7}$$

The formulation in (7) stems from the experience that a field-dependent mobility $\mu(E)$ results in a more accurate description of the heat flow than an energy-dependent one.

The collision terms, which are denoted by the subscript "coll," consist of several contributions due to lattice scattering and collision between mobile carriers. Since processes of generation and recombination are not present for unipolar transport, the effect of collision can be described by the expressions

$$\left(\frac{\partial n}{\partial t}\right)_{\rm coll} = 0 \tag{8}$$

$$\left(\frac{\partial n \vec{v}}{\partial t}\right)_{\rm coll} = -n \frac{\vec{v}}{\tau_m(w)} \tag{9}$$

$$\left(\frac{\partial n w}{\partial t}\right)_{\rm coll} = -n \frac{w - w_0}{\tau_w(w)}. \tag{10}$$

In order to fit the unknown relaxation time constants in (9) and (10) to stationary MC results for homogeneous material, we set

$$\tau_m(w_{\rm ss}) = \frac{m^*_{\rm ss} v_{\rm ss}}{q E_{\rm ss}} \tag{11}$$

$$\tau_w(w_{\rm ss}) = \frac{w_{\rm ss} - w_0}{q v_{\rm ss} E_{\rm ss}}. \tag{12}$$

All steady-state values that are denoted by the subscript ss, as well as m^*, are assumed to depend on mean energy $w(E_{\rm ss})$. The solution of the resulting system of partial differential equations is accomplished by a fully implicit, decoupled, yet unconditionally stable finite-difference scheme. A special discretization of Poisson's equation for one-dimensional structures ensures unconditional stability of the solution algorithm and allows large time steps to be used [7].

Results of the present model are in close agreement with those of several CA simulations of Gunn devices in the millimeter-wave range. In order to investigate and to optimize the different device properties with respect to output power and device impedance, extensive simulations are necessary. These are performed under impressed bias voltage conditions at the device terminal which, for harmonic-mode operation, can be written as

$$V(t) = V_0 + V_1 \sin(2\pi f_1 t) + V_2 \sin(2\pi f_2 t + \varphi). \tag{13}$$

In a second step for optimized device structures, consistent oscillator simulations can be performed by embedding the device into a lumped-element circuitry.

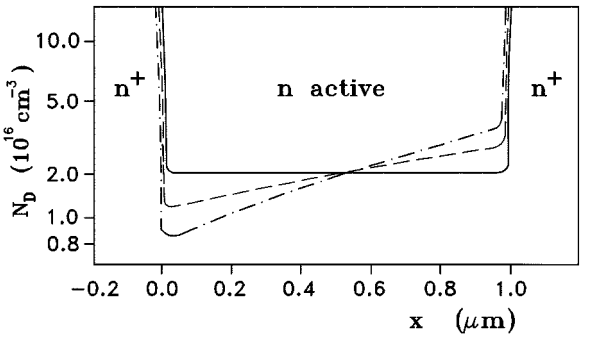

Fig. 2. Schematic profiles of Gunn devices with constant and linearly graded active layer.

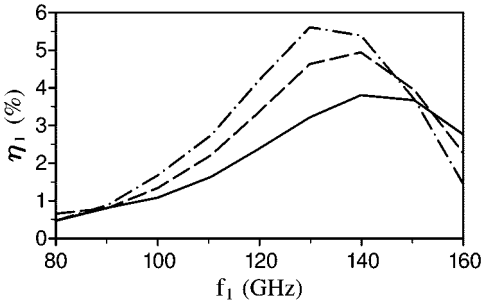

Fig. 3. Efficiency for fundamental-mode operation $V_0 = 4.5$ V, $V_1 = 2.0$ V graded doping profiles, as defined in Fig. 2.

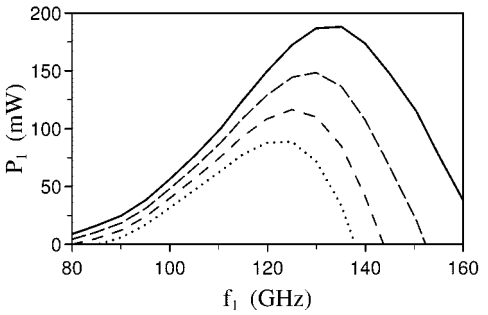

Fig. 4. Degradation of output power due to series resistance: $R_s = 0.0\ \Omega$ (———), 0.3Ω (- - -), 0.6Ω (– – –), 0.9Ω (· · · · · · · · ·), fundamental-mode operation: $V_0 = 4.5$ V, $V_1 = 2.0$ V, graded doping profile: (– · – · –), as defined in Fig. 1.

III. Gunn Devices

Since the evolution of the electron–charge instability is strongly influenced by the doping profile, the general limitation

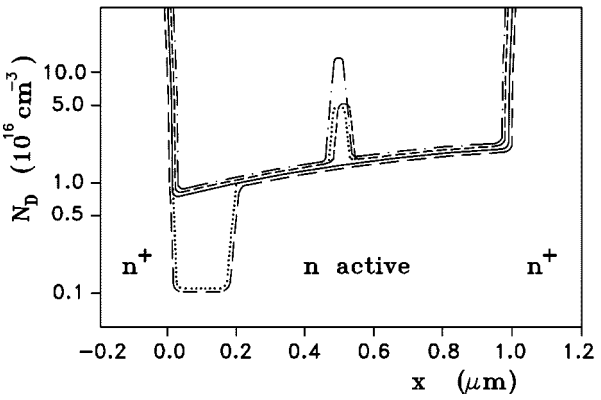

Fig. 5. Doping profiles under investigation. Graded profile: (———) [1], cathode notch profile: (— — —), mesa profiles: (- - - - - -), (— · — · —): combination of cathode notch, and mesa profile: (· · · · · · · · ·).

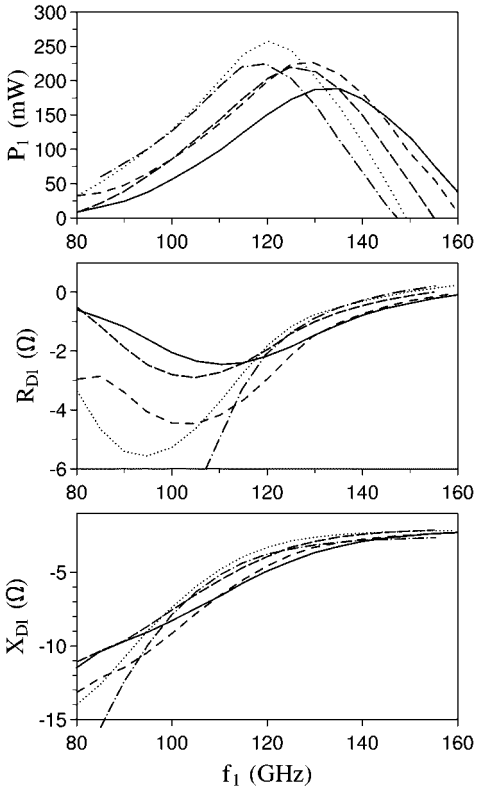

Fig. 6. Output power and device impedance for fundamental-mode operation $V_0 = 4.5$ V, $V_1 = 2.0$ V doping profiles, as defined in Fig. 5.

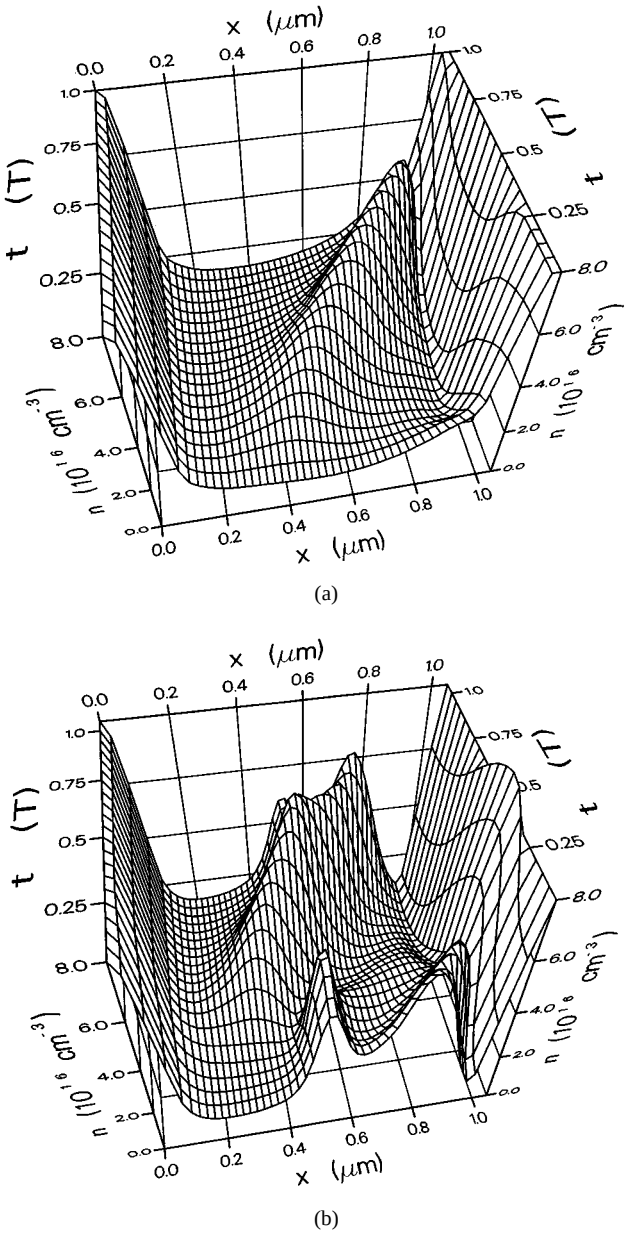

Fig. 7. Electron density evolution over one period for: (a) graded profile: (——— Fig. 5) [1] and (b) mesa profile: (— · — · — Fig. 5), fundamental-mode operation: $V_0 = 4.5$ V, $V_1 = 2.0$ V.

of Gunn devices in length to 1 μm is not evident. Nevertheless, the common active length of all devices has been set to 1 μm in order to demonstrate the effect of impurity modulation. In a first step, the effect of a graded doping density from cathode to anode (Fig. 2) has been investigated for fundamental-mode operation $(V_2 = 0)$. It is expected that a stimulation of the electron charge instability growth takes place, which results in higher output power and efficiency. This is confirmed by the simulation as has been depicted in Fig. 3. In comparison with a constant doping density, the graded profile $(-\cdot-\cdot-)$ exhibits twice the device efficiency for fundamental-mode operation at 130 GHz. It should be noted that the device diameter for different profiles is adjusted to result in equal dc-power dissipation of $P_0 \approx 4.5$ W for given ac conditions, and that the device temperature is assumed to be $T = 400$ K. Furthermore, losses due to contacts and bulk resistance are neglected in the present analysis, although these losses can, in practical circuits, lead to drastic performance degradation. As an example, in Fig. 4, different series resistances have been assumed, which can completely suppress output power extraction, especially at higher frequencies.

As a modification of graded doping profiles that have been successfully designed, fabricated, and tested around 130 GHz in the work described in [3], a doping notch at the cathode and/or a doping mesa located in the center of the active region have been added (Fig. 5). The former creates an above-threshold electrical field near the cathode, which insures exclusive nucleation and launching of dipole layers from the cathode, whereas the latter

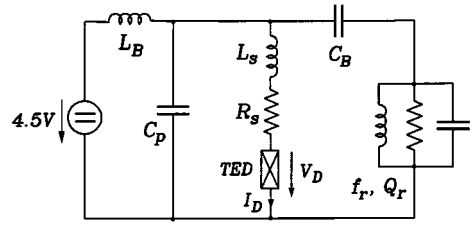

(a)

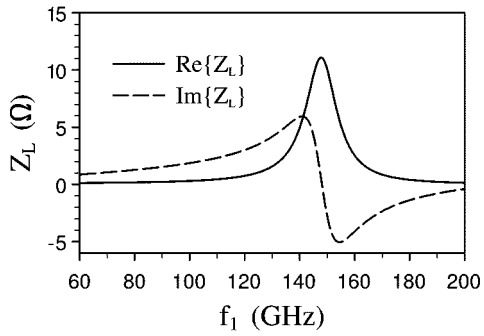

(b)

Fig. 8. (a) Oscillator circuit for consistent simulation. (b) Typical load impedance Z_L at the device terminal.

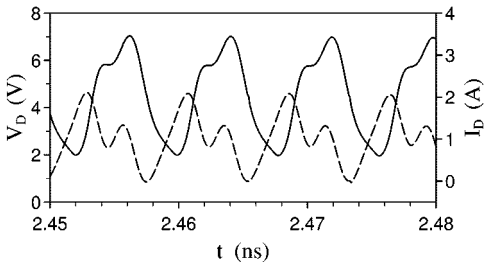

Fig. 9. Simulated terminal voltage and current characteristic for InP Gunn device (graded doping) operating at 128 GHz ($V_0 = 4.5$ V).

results in a modulation of the strong fundamental current oscillation in order to produce a higher quantity of harmonic output power [8].

IV. Results

For all the doping profiles of Fig. 5, both fundamental- and harmonic-mode simulations have been performed. Fig. 6 shows the RF power generation and device impedance for fundamental-mode operation under impressed terminal voltage conditions. Taking into account the inclusion of series losses, the output power for the graded profile (solid line) is in close agreement with the measured results reported in [3]. Furthermore, Fig. 6 clearly depicts the increase in RF power for the modified doping profiles that corresponds to an increase in efficiency up to 6% at 120 GHz. The charge instability evolution over one period of oscillation for the graded profile and mesa profile, respectively, is illustrated in Fig. 7. In comparison, premature instability appearance can be observed for the mesa profile, which is advantageous for efficient power generation.

The previous investigations have assumed a device that is driven by an impressed sinusoidal voltage at the device terminal. However, the corresponding results are only transferable to oscillator circuits if both the driving condition, which had to be assumed before, and the load impedance are realistic. Especially for harmonic-mode operation, different driving conditions (impressed voltages or impressed currents) lead to significantly differing device performance. Due to that, consistent simulations have been performed by incorporating the device into a simple network of lumped elements, as depicted in

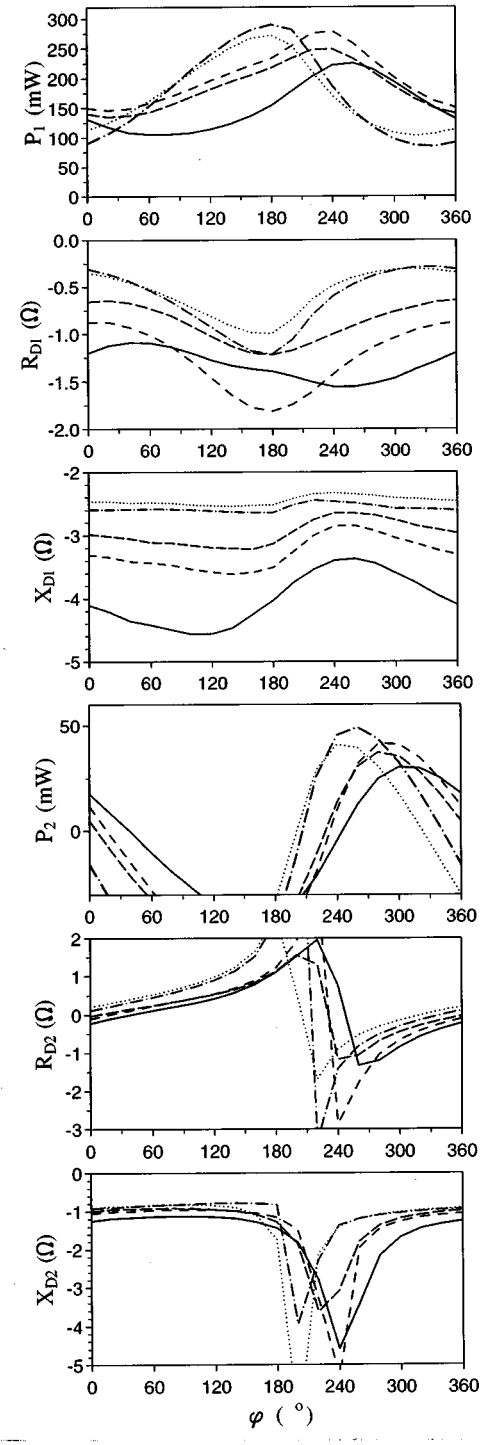

Fig. 10. Harmonic-mode operation $f = 130/260$ GHz, $V_0 = 4.5$ V, $V_1 = 2.0$ V, $V_2 = 0.5$ V corresponding doping profiles, as defined in Fig. 5, φ as defined in (13).

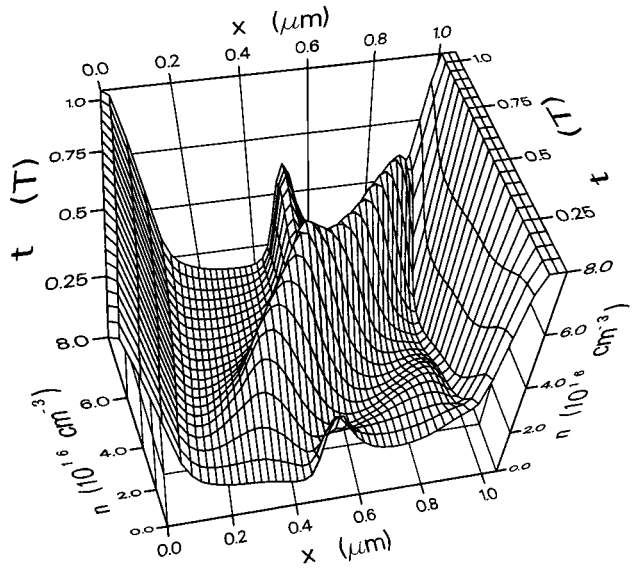

Fig. 11. Electron density evolution over one period for mesa profile: (—·—·— Fig. 5), harmonic mode: $V_0 = 4.5$ V, $V_1 = 2.0$ V, $V_2 = 0.5$ V, $\varphi = 260°$.

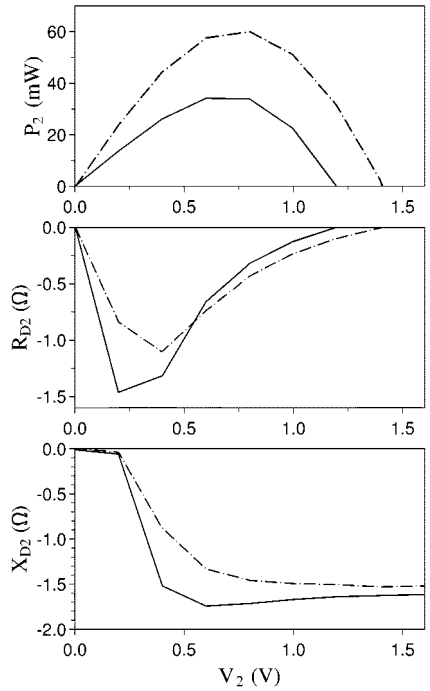

Fig. 12. Harmonic-mode operation $f = 130/260$ GHz, $V_0 = 4.5$ V, $V_1 = 2.0$ V, graded profile: (——— Fig. 5) $\varphi = 290°$, mesa profile: (—·—·— Fig. 5), $\varphi = 260°$.

Fig. 8(a) (fundamental mode). The circuit consists of a constant dc voltage source, three parasitic elements R_s, L_s, and C_p, corresponding to the device package, and a parallel resonant circuit of quality factor Q_r and resonant frequency f_r, respectively, which result in a load impedance characteristic at the device terminal, as shown in Fig. 8(b). The oscillator analysis is based on a time-domain approach that simultaneously performs device and circuit simulation, which are explicitly coupled by a case-sensitive modification of Newton–Raphson iterations. As an example, for a dc voltage of 4.5 V and a load impedance Z_L according to Fig. 8(b), oscillator simulations of a graded doping profile device have been performed up to steady state. Fig. 9 shows the resulting voltage and current waveform at the device terminal, the fundamental output power of which is 238 mW at 128 GHz.

For harmonic-mode operation, power extraction at 260 GHz can be expected only in a limited range of the phase angle φ, as is shown in Fig. 10. Thus, a careful adjustment of the load impedance characteristic at both fundamental and harmonic frequency must be fulfilled in practical oscillator circuits. As an additional result, higher harmonic power levels are corresponding with mesa profiles, the harmonic device resistance of which is larger in magnitude in comparison with that of the graded profile. This is an important result since series losses due to bulk resistance and skin effect are responsible for a dramatic degradation of the power generation capability at frequencies above 150 GHz. The charge instability evolution in Fig. 11 indicates that the dipole layer is modulated when it drifts through the doping mesa. This property confirms the appearance of a higher quantity of harmonic output power. Finally, Fig. 12 compares graded and mesa profile devices as a function of the second harmonic voltage V_2.

V. Conclusions

InP Gunn devices of various doping profiles have theoretically been investigated for fundamental- and harmonic-mode operation at frequencies up to 260 GHz. The results are based on an efficient and accurate HD simulator, which analyzes the device under impressed terminal voltage conditions. In comparison with state-of-the-art graded profile diodes, improved performance is demonstrated for modulated impurity-concentration devices for both modes of operation.

Acknowledgment

The author is indebted to M. Curow and K. Schünemann for helpful discussions and to D. Liebig for supplying the steady-state transport coefficients.

References

[1] H. Eisele and G. I. Haddad, "D-band InP Gunn devices with second-harmonic power extraction up to 290 GHz," *Electron. Lett.*, vol. 30, no. 23, pp. 1950–1951, Nov. 1994.

[2] A. Rydberg, "High efficiency and output power from second- and third-harmonic millimeter-wave InP-TED oscillators at frequencies above 170 GHz," *IEEE Electron Device Lett.*, vol. 11, pp. 439–441, Oct. 1990.

[3] H. Eisele and G. I. Haddad, "High-performance InP Gunn devices for fundamental-mode operation in D-band (110–170 GHz)," *IEEE Microwave Guided Wave Lett.*, vol. 5, pp. 385–387, Nov. 1995.

[4] J. D. Crowley *et al.*, "140 GHz indium phosphide Gunn diode," *Electron. Lett.*, vol. 30, no. 6, pp. 499–500, Mar. 1994.

[5] D. Liebig and K. Schünemann, "Cellular automaton particle simulation and sensitivity analysis of GaAs-MITATT-diodes for operation at 200 GHz," *Int. J. Electron. Commun.*, vol. 52, no. 5, pp. 329–334, May 1998.

[6] K. Bløtekjær, "Transport equations for electrons in two-valley semiconductors," *IEEE Trans. Electron Devices*, vol. ED-17, pp. 38–47, Jan. 1970.

[7] M. Curow, "Konsistente simulation von millimeterwellen-oszillatoren mit Gunn-elementen und IMPATT-dioden," Ph.D. dissertation, Arbeitsbereich Hochfrequenztechnik, Technical Univ. Hamburg-Harburg, Hamburg, Germany, Mar. 1996.

[8] S. H. Jones, G. B. Tait, and M. Shur, "Modulated-impurity-concentration transferred-electron devices exhibiting large harmonic frequency content," *Microwave Opt. Technol. Lett.*, vol. 5, pp. 354–359, July 1992.

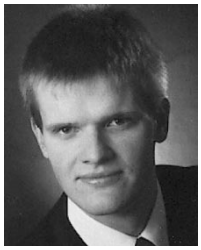

Rolf Judaschke (M'93) was born in Lübeck, Germany, in 1965. He received the Dipl.-Ing. degree in electrical engineering from the Technische Universität Braunschweig, Braunschweig, Germany, in 1991, and the Dr.-Ing. degree from the Technische Universität Hamburg-Harburg, Hamburg, Germany, in 1997.

Since 1991, he has been a Research Assistant at the Technische Universität Hamburg-Harburg, where he is currently involved in the investigation of millimeter-wave solid-state oscillators, radars, and power-combining techniques.